Quantum non-Markovian noise in randomized benchmarking of spin-boson models

Srilekha Gandhari [1,*] and Michael J. Gullans [1,2,†]

[1] *Joint Center for Quantum Information and Computer Science, NIST/University of Maryland, College Park, Maryland 20742, USA*

[2] *National Institute of Standards and Technology, Gaithersburg, Maryland 20899, USA*

(Received 21 April 2025; accepted 24 February 2026; published 24 April 2026)

In non-Markovian systems, the current state of the system depends on the full or partial history of its past evolution. Owing to these time correlations, non-Markovian noise violates common assumptions in gate characterization protocols such as randomized benchmarking and gate-set tomography. Here, we perform a case study of the effects of a quantum non-Markovian bath on qubit randomized benchmarking experiments. We consider a model consisting of qubits coupled to a multimode bosonic bath. We apply unitary operations on the qubits, interspersed with brief interactions with the environment governed by a Hamiltonian. Allowing for non-Markovianity in the interactions leads to clear differences in the randomized benchmarking decay curves in this model, which we analyze in detail. The Markovian model's decay is exponential as expected, whereas the model with non-Markovian interactions displays a much slower, almost polynomial, decay. We develop efficient numerical methods for this problem that we use to support our theoretical results. These results inform efforts on incorporating quantum non-Markovian noise in the characterization and benchmarking of quantum devices.

DOI: 10.1103/z8zh-n1hl

I. INTRODUCTION

Noise characterization is central to the operation of quantum devices and processors. The large dimension of Hilbert space of many-body quantum systems, coupled with the sensitivity of quantum states to measurements, makes benchmarking quantum devices a complex task. There are several methods to characterize quantum operations, with varying degrees of detail, to assess whether they are functioning as intended. Randomized benchmarking (RB) is a particularly common technique due to its resource efficiency and insensitivity to state preparation and measurement (SPAM) errors [1–7].

A key assumption prevalent in studies of quantum information is that of *Markovian* noise. Also referred to as time-independent or i.i.d. noise, Markovianity is a property of a stochastic process where the future of a system is dependent only on its current state, irrespective of how it reached there. In other words, Markovian noise does not carry any temporal correlations with its past. This vastly simplifies the mathematics involved and, in many cases, has proved to be a reasonable approximation so far. But recent studies have shown the limitations of this assumption and the need to study correlated noise [8–14]. Although the effects of classical correlations over time have been studied [15–17], they do not capture the effects of having a quantum bath capable of entanglement with the system, which is a setting that is gaining greater emphasis [18–22]. One widely used approach to mitigate non-Markovian noise is dynamical decoupling [23–26], where tailored pulse sequences are applied to average out slow environmental fluctuations. For a fully general and operational description of non-Markovian dynamics, the process tensor framework [11,27] provides a complete characterization by reconstructing multitime correlations from a tomographically complete set of input control operations. However, these frameworks provide a general and abstract way to deal with non-Markovianity and give limited idea about the dynamics until fully equipped with details of the underlying physical model. In this work, we instead study the effects of non-Markovian noise on RB using an exactly solvable model, which allows us to isolate and interpret the dynamical features that give rise to deviations from standard Markovian RB decay.

Here, we consider RB of qubit systems coupled to a non-Markovian bosonic bath. We provide an efficient algorithm for calculating the final state of the system after a given time. We then show that quantum non-Markovian effects have a dramatic effect on the fidelity decay by modifying it from a simple exponential to a power-law times exponential. In our model, the system and the bath interact through a fixed spin-boson Hamiltonian [28–30] and correlations are generated by the virtue of the bath having dynamics at a slower timescale than the system. We find that there are strong qualitative differences in the RB decay when comparing Markovian and non-Markovian limits of the model. We trace the origin of the non-Markovian dynamics to heating dynamics of the bath arising from coupling to the driven system. In addition, we identify a simple fingerprint for the presence of non-Markovian noise in RB based on the distinguishability between two orthogonal input states to the same RB circuit. These results serve as important guides in the quest

*Contact author: sgandha@sandia.gov

†Contact author: mgullans@umd.edu

to characterize and control non-Markovian noise in quantum devices.

II. BACKGROUND AND RELATED WORKS

A. Randomized benchmarking

RB was originally created to extract the depolarizing parameter of time- and gate-independent noise within a gate set, and has since been generalized to a broad range of other cases [1–7]. The gate set $\mathcal{G}$ twirls, or averages, the noise channel and is required to form a finite group. In practice, it is typically chosen to be the Clifford group, the group of unitaries that map Pauli operators to Pauli operators up to a global phase. [31] The Clifford group is especially significant because it forms a unitary 2-design and admits fault-tolerant implementations across many quantum architectures.

Any gate-independent noise channel Λ twirled over the Clifford group results in a depolarizing channel. For a d-dimensional system and any quantum state ρ, twirling a noise channel Λ uniformly over all unitaries (or over a unitary 2-design such as the Clifford group) yields

$$\mathbb{E}[\mathcal{U}^{-1} \circ \Lambda \circ \mathcal{U}(\rho)] = p\,\rho + (1-p)\frac{\mathbb{I}}{d}. \tag{1}$$

Using RB, we can extract the depolarizing parameter p of the noisy gate set, assuming each noisy gate is modeled as an ideal gate followed by a gate- and time-independent noise channel [32,33].

Recent studies have shown the limitations of the Markovian assumption and the need to study correlated noise [8–14].

B. Spin-boson models

We consider an open quantum system with a bosonic bath. A bosonic state is a continuous-variable quantum state that can be made of multiple *modes*, akin to having multiple qubits in a discrete-variable system. Each mode in our bosonic bath is modeled as a quantum harmonic oscillator, consisting of a ladder of occupational states and equipped with the annihilation and creation operators a and $a^\dagger$. Bosonic environments are particularly relevant in modern quantum experiments, as most leading platforms—such as superconducting circuits, trapped ions, and neutral-atom arrays—use electromagnetic fields both as control mechanisms and as dominant channels through which the system exchanges energy and information with its surroundings. A simple Hamiltonian of such a bath, with noninteracting modes, is given by

$$H_{\text{bath}} = \sum_i \omega_i a_i a_i^\dagger, \tag{2}$$

where summation is over all the modes and $\{\omega_i\}_i$ are the respective angular frequencies. Depending on the noise profile, one can assume the frequencies drawn from different distributions. Although each mode contains an infinite number of occupational states, we will see later that in our numerical simulations we impose a practical cutoff to keep the dimension finite.

We consider a set of qubits as our system with the ability to initialize it in the computational zero state, implement unitary gates, and measure in the computational basis. Though the rest of our analysis is platform-agnostic and applies to all qubit encodings, we adopt the two-level spin-qubit formalism with a system Hamiltonian H_{sys} as a convenient and standard representation for carrying out explicit calculations. This spin-qubit system interacts with the bosonic bath via a Hamiltonian H_{int}:

$$H_{\text{int}} = \sum_i \sum_{j=1}^{n} g_i \sigma_x^{(j)} x_i, \tag{3}$$

where $\{g_i\}_i$ are the interaction strengths of each bosonic mode, the position and momentum operators $\{x_i, p_i\}$ of the ith mode are defined in terms of its annihilation and creation operators as $\frac{a_i \pm a_i^\dagger}{\sqrt{2}}$, respectively, and the summation over j is over all the n qubits present in the system.

The theoretical analysis of RB is typically carried out at the circuit level, where one works with abstract quantum operations rather than, but motivated by, the physical details of the underlying hardware. In this abstraction, microscopic features—such as the specific system Hamiltonian H_{sys}, native interactions, or control mechanisms—are often ignored. This simplification is justified in the Markovian setting as any gate-independent noise channel is twirled into a depolarizing channel under the Clifford group, making the details of the physical evolution inconsequential to the RB decay model. One can interpret it as observing the dynamics from a constant system frame [34,35].

However, choosing to ignore H_{sys} is not so straightforward in the presence of gate-dependent or non-Markovian interactions. If the random unitaries are sampled from the Haar measure, then using the left or right invariance of the Haar measure, one can, on average, *absorb* H_{sys} into the random unitaries [36]. But one typically samples the unitaries from the Clifford group in RB experiments, which does not possess the former invariance property. In this work, we choose to ignore H_{sys} irrespective of the nature of interactions and the gate set the unitaries are sampled from—a step that results in focusing on the incoherent errors that act on the system and not the coherent ones [37–39].

Hence, for a single qubit coupled to m bosonic modes, the complete system-environment Hamiltonian is

$$H = \sum_{i=1}^{m} g_i \sigma_z x_i + \frac{\omega_i}{2}\left(x_i^2 + p_i^2\right). \tag{4}$$

This can be written in terms of projectors onto the $|0\rangle$ and $|1\rangle$ subspaces of the qubit as

$$H = P_0 \otimes H_0 + P_1 \otimes H_1 = H_0 \oplus H_1, \tag{5}$$

where

$$H_{0/1} = \sum_i \frac{\omega_i}{2}\left(\left(x_i \pm \frac{g_i}{\omega_i}\right)^2 + p_i^2\right) - \frac{g_i^2}{2\omega_i}. \tag{6}$$

The evolution operator for a time duration Δt can therefore be written as

$$\mathcal{H} \equiv e^{-iH\Delta t} = P_0 \otimes e^{-iH_0\Delta t} + P_1 \otimes e^{-iH_1\Delta t} \tag{7}$$

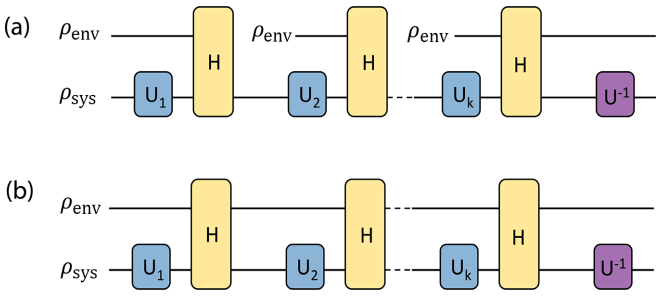

FIG. 1. Circuit representation of (a) Markovian model where a qubit system ρ_{sys} is coupled to a renewing environment ρ_{env}. (b) Non-Markovian model with a persistent environment ρ_{env} that continues to couple to the qubit system ρ_{sys} without refreshing. In both cases, we initialized the environment in the same thermal state for our numerical simulations. All the random unitaries are drawn from the Clifford group and $U^{-1} = (U_k \cdots U_1)^{-1}$. The time interval between the random unitary gates is Δt. The interactions are through an evolution unitary $U = e^{-iH\Delta t}$ governed by the Hamiltonian H.

and define the evolution map $\mathcal{E}_H(\cdot) = \mathcal{H} \cdot \mathcal{H}^\dagger$. The same can be extended to multiqubit systems, which we discuss in Sec. IV E. We note that the choice of the Z basis for the coupling term is arbitrary in this model.

As shown in Fig. 1, we consider a circuit model where the qubit system ρ_s interacts with a multimode bosonic bath (ρ_{env}) through a Hamiltonian $\mathcal{H}$, interspersed with the unitary operations $U_1, \ldots, U_k$. We define the unitary channel acting only on the system as $\mathcal{U}_i(\cdot) = (U_i \otimes \mathbb{I}) \cdot (U_i^\dagger \otimes \mathbb{I})$.

In the Markovian setting, the environment is constantly refreshed in before every interaction with the system, whereas in the more general non-Markovian case, the environment continues to evolve without losing any information. The difference between the average overlap $\langle \rho_s | \rho_{final} \rangle$ of the two cases tells us the extent of non-Markovianity, that is, how much information is flowing back from the environment to affect the future of the system. We justify our models in the next section. Let us justify our constructions in the next section.

III. MARKOVIAN AND NON-MARKOVIAN MODELS

A stochastic process is an evolution of a random variable over time, and is said to be Markovian if the next value the random variable takes depends only on its current value and not its history. It is said to be non-Markovian if its past values also influence the next step. Mathematically, for a random variable X over the time index t, for a Markov process one can write the conditional probability

$$\Pr\left(X_{t_k} \middle| X_{t_{k-1}}, \ldots, X_{t_1}\right) = \Pr(X_{t_k} | X_{t_{k-1}}) \quad \forall\, t_1 \leqslant \cdots \leqslant t_{k-1} \leqslant t_k. \tag{8}$$

This classical definition of Markovianity is difficult to extend to quantum systems because of the impossibility of knowing the state of the system at every time step without collapsing it. One rather looks at the quantum maps that act on the quantum systems and classify their behavior. A quantum channel family $\{\Lambda_i\}$ is CP-divisible [40] if for all $m \geqslant n$ there exists a CPTP map $\Lambda_{m,n}$ such that

$$\Lambda_n = \Lambda_{n,m} \circ \Lambda_m. \tag{9}$$

Our model in Fig. 1(a) is CP-divisible and follows the semigroup property, and can therefore be proved Markovian. The action of one layer includes a random unitary U_i acting on the system, followed by the interaction with the environment and the inverse unitary acting again only on the system. Mathematically, this can be written as

$$\mathcal{E}_{M,\rho_{env}}(\rho_s, \mathcal{U}_i) = \mathrm{tr}_E[\mathcal{U}_i^\dagger \circ \mathcal{E}_H \circ \mathcal{U}_i(\rho_s \otimes \rho_{env})]. \tag{10}$$

The state of the system at time t_n can be described as the action of composition of maps from time t_m:

$$\rho_{sys,n} = \bigcirc_{i=m}^{n} \mathcal{E}_{M,\rho_{env}}(\rho_{sys,m}), \tag{11}$$

thereby satisfying Eq. (9). However, the same cannot be done in the case of our model in Fig. 1(b) with a persistent environment, which has a capacity to carry temporal correlations. We propose this is a non-Markovian model and verify our claim in Sec. V through a distinguishability test.

IV. STATE EVOLUTIONS

A. Markovian evolution

In our Markovian model, as shown in Fig. 1(a), the environment resets before every interaction with the system, thus carrying no information about the system with itself and preventing non-Markovian correlations. We showed that the average sequence fidelity in this case is an exponential decay with depth, which is consistent with the existing literature. We calculated this for a depth k circuit by assuming a product initial state, applying the Markovian map k times, and averaging the unitaries over the Clifford group. It is given by (see Appendix B)

$$f_k^M(\rho_s, \rho_{env}) = \frac{1}{2} + \frac{1}{2}\left(\frac{1 + 2\ \mathrm{tr}\,(\cos(2gx\Delta t)\rho_{env})}{3}\right)^k. \tag{12}$$

B. Non-Markovian evolution

Our non-Markovian model, as shown in Fig. 1(b), has a continuing environment coupled to the system. If the initial state is assumed to be in a product state $\rho_{in} = \rho_s \otimes \rho_{env}$, the average final state of a depth k circuit is

$$\mathbb{E}_U[\rho_{s,k}] = \mathrm{tr}_E(\mathbb{E}_U[\mathcal{U}^{-1} \circ \mathcal{E}_H \circ \mathcal{U}_k \cdots \circ \mathcal{E}_H \circ \mathcal{U}_1\,(\rho_s \otimes \rho_{env})]), \tag{13}$$

where each of the gates $\{U_i\}_{i=1}^k$ is sampled uniformly randomly from the Clifford group, the expectation value $\mathbb{E}_U$ is over all U_i, and the evolution map $\mathcal{E}_H$ is as defined earlier.

Using Eq. (7), we denote the trajectories created by the action of the projectors using k-length binary strings $\mathbf{p}$, $\mathbf{q}$, where $p_i, q_i \in \{0, 1\}\, \forall\, i = 1, 2, \ldots, k$. Therefore, we can express the final state as a sum of all possible trajectories

$$\mathbb{E}_U[\rho_{s,k}] \equiv \sum_{\mathbf{p},\mathbf{q} \in \{0,1\}^{\otimes k}} \mathbb{E}_U\big[U^{-1} P_{p_k} U_k \cdots P_{p_1} U_1 \rho_s U_1^\dagger \times P_{q_1} \cdots U_k^\dagger P_{q_k} U^{-1\dagger}\big] \times \mathrm{tr}\,(\mathcal{H}(\mathbf{p})\,\rho_{env}\,\mathcal{H}(\mathbf{q})), \tag{14}$$

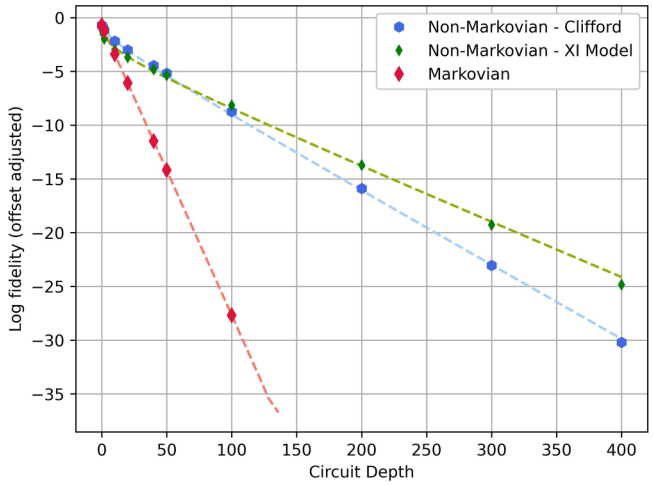

FIG. 2. Single qubit decay of randomized benchmarking output with circuit depth k, along with their numerical fits. Non-Markovian evolution with the Clifford gate set (blue hexagons) fits a subexponential of the form $\frac{1}{2} + Ak^{-1/3}e^{-ck}$, whereas Markovian evolution with the same gate set (red diamonds) fits a exponential decay $\frac{1}{2} + Ae^{-ck}$. Non-Markovian decay with the $\{X, \mathbb{I}\}$ gate set (green diamonds) fits $\frac{1}{2} + Ak^{-1/2}e^{-ck}$. The plot shows $\ln(f_k - \frac{1}{2})$ vs depth k. The environments are initialized in thermal states with interaction strength $g = 4$, bosonic frequency $\omega = 10$, temperature $T = 10^{-10}$, and gate time $\Delta t = 0.1$ in dimensionless units.

where evolution of the environment along a trajectory is tracked with the help of $\mathcal{H}(\mathbf{x}) = e^{-iH_{x_k}\Delta t} \cdots e^{-iH_{x_1}\Delta t}$. As explained in Appendix A, we can compute the average over the unitaries using methods of Haar integration, and the *average sequence fidelity* is shown to be

$$f_k^{NM}(\rho_s, \rho_{\text{env}}) = \frac{1}{2} + \frac{1}{2}\frac{1}{6^k}\left(\sum_{\mathbf{p},\mathbf{q}} 2^{d(\mathbf{p},\mathbf{q})}\,\text{tr}\left(\mathcal{H}(\mathbf{p})\,\rho_{\text{env}}\,\mathcal{H}^\dagger(\mathbf{q})\right)\right), \tag{15}$$

where $d(\mathbf{p}, \mathbf{q})$ is the Hamming distance between $\mathbf{p}$ and $\mathbf{q}$. Note that $\sum_{\mathbf{p},\mathbf{q}} 2^{d(\mathbf{p},\mathbf{q})} = 6^k$ and therefore in the absence of any interactions with the bath, the fidelity is always 1.

Numerical implementation. In order to avoid the exponentially growing number of trajectories in the analytical expression in Eq. (14), we developed a numerical method that is far more efficient in time. With every Hamiltonian interaction, there is a step of projecting onto the 4^n computational basis states of the space of operators $\mathcal{B}(\mathcal{H})$. After averaging, we are left with 4^{2n} terms (see Appendix A), and the process continues. Knowing the state after every step explicitly in our numerics allows us to circumvent this by regrouping the 4^{2n} terms into 4^n basis states, and thus always limiting the number of terms to 4^n. This removes the need for any approximations and computes the exact average sequence fidelity of the non-Markovian model.

As mentioned earlier, we imposed a reasonable occupational-number cutoff for the environment that does not impact system dynamics in all our numeric implementations.

The above two cases are illustrated in Fig. 2. Crucially, it leads us to the observation that RB decay of non-Markovian systems does not follow an exponential trend, and can be explained as a power-law times exponential, with respect to depth. The subexponential behavior is especially apparent at smaller depths and provides us with a powerful signature of temporal correlations—one that can be used to identify and characterize such noise. In the figure, non-Markovian decay is compared with the Markovian case, which exhibits exponential RB decay as proved.

C. Dependence on gate set

We analyze the fidelity decay for our models by considering a gate set different from the previous examples. In randomized benchmarking, the choice of the gate set determines the group over which the noise channel is twirled, and the representation structure of this group directly dictates the form of the average sequence fidelity decay. If the gate set's action on the traceless operators' subspace decomposes into multiple irreducible representations, the twirled noise channel acquires multiple eigenvalues, leading to a multiexponential decay. In contrast, the Clifford group acts irreducible on the traceless Pauli operators (treating all Paulis uniformly), yielding a single decay parameter and therefore a single-exponential decay [41].

Here, we consider a different gate set from the Clifford group and show how to obtain the averaged final state in a non-Markovian setting, when one cannot use Haar averaging tools. We consider a single-qubit system initialized in the $|+\rangle$ state and the unitary gates uniformly sampled from $\{X, \mathbb{I}\}$. Both the X and $\mathbb{I}$ gates leave the $|+\rangle$ state unchanged, eliminating the need for an inverse. Using the anticommutation relation $\{X, Z\} = 0$, the action of X gate on the evolution operator is

$$\begin{aligned} X\,e^{-iHt} &= X\,e^{-i(g(a+a^\dagger)Z + \omega a a^\dagger \mathbb{I})\Delta t} \\ &= e^{-i(-g(a+a^\dagger)Z + \omega a a^\dagger \mathbb{I})\Delta t}\,X. \end{aligned} \tag{16}$$

Using this, in Appendix C we showed how to compute the average final state of a non-Markovian circuit with this gate set. The Markovian case can be worked out as in Appendix B.

D. Behavior of environment modes

To understand the change in the environment throughout this process, we look at how the average photon number of environment, which begins in a thermal state, changes with the depth of the circuit. Starting with Eq. (13), and an initial state $\rho_{\text{in}} = \rho_s \otimes \rho_{\text{env}}$, the average photon-number after k layers is

$$\begin{aligned} \langle n_k \rangle &= \mathbb{E}\left[n_k^{\text{env}}(\rho_{\text{in}})\right] \\ &= \sum_{\mathbf{p},\mathbf{q}\in\{0,1\}^{\otimes k}} \text{tr}\left(\mathbb{E}_U[\mathcal{M}_k]\right)\,\text{tr}\left(a^\dagger a\,\mathcal{H}(\mathbf{p})\rho_{\text{env}}\mathcal{H}^\dagger(\mathbf{q})\right) \\ &= \sum_{\mathbf{p}\in\{0,1\}^{\otimes k}} \frac{1}{2^k}\,\text{tr}\left(\rho_s\right)\,\text{tr}\left(a^\dagger a\,\mathcal{H}(\mathbf{p})\rho_{\text{env}}\mathcal{H}^\dagger(\mathbf{p})\right). \end{aligned} \tag{17}$$

On plotting this result, we observed that $\langle n \rangle$ saturates to a value independent of the parameters g, ω, t. Figure 3 shows that $\langle n \rangle$ has a strong dependence on the cutoff point of the occupational number of the environment, indicating that the system is undergoing continuous heating in this model. The slow overall rate of the heating compared to a

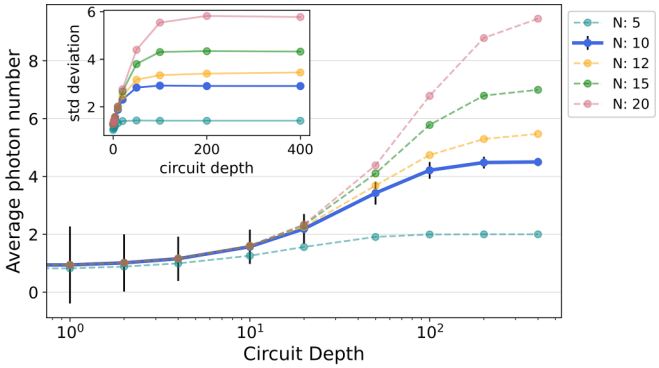

FIG. 3. Average photon number of the environment initialized to a thermal state, starting at $\langle n\rangle \approx 0.87$, plotted against different occupational-number cutoffs (N) of the environment mode. We observed that $\langle n\rangle$ does not depend on any of the other parameters of the system or environment. It saturates to a value of around 4.5 for a cutoff value of $N = 10$; see text for discussion. $g = 4$, $\omega = 10$, $T = 10^{-10}$, and $\Delta t = 0.1$ in dimensionless units for all the curves. Inset: Variance of the photon number at different values of N.

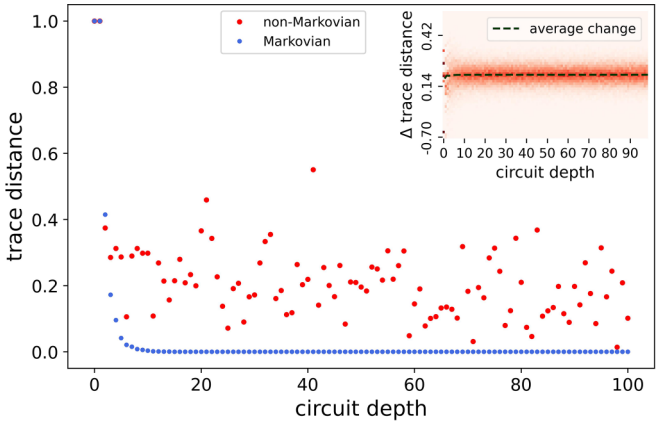

FIG. 4. Difference in trace distance between the evolutions beginning in the orthogonal states $|0\rangle$ and $|1\rangle$, plotted with respect to depth for a random circuit, for both Markovian and non-Markovian models. $g = 4$, $\omega = 10$, $T = 10^{-10}$, and $\Delta t = 0.1$ in dimensionless units. Inset: Distribution of the change in trace distance for non-Markovian circuits. The histograms, collected for 10^3 random Clifford circuits, are displayed as color plots.

Markovian system qualitatively explains the slower decay of the RB output in the non-Markovian case.

E. Multiqubit systems and multimode baths

Our results extend to, and result in, similar trends, in multiqubit systems and systems interacting with multimode baths. One can write a general Hamiltonian for n qubits and m modes as follows:

$$H = \sum_{i=1}^{m} \omega_i a_i^\dagger a_i + \sum_{j=1}^{n}\sum_{i=1}^{m} g_{ij}\sigma_{zj}(a_i + a_i^\dagger) = \bigoplus_{p\in\{0,1\}^{\otimes n}} H_p. \tag{18}$$

Using the weighted sum of a bit string $w(q) \equiv \sum_{j=1}^{n}(-1)^{q_j}$,

$$H_p = \sum_{i=1}^{m} \omega_i a_i^\dagger a_i + w(p)\, g_{ij}(a_i + a_i^\dagger). \tag{19}$$

As before, we can assume that we begin in a product state $\rho_{\rm SE} = \rho_s \otimes \rho_{\rm env}$, and apply a sequence of n-qubit unitary operations $U_1, \ldots, U_k, U_{\rm inv}$, where $d = 2^n$, $U_i \in \mathbb{U}_d$, and $U_{\rm inv} = (U_1 \cdots U_k)^{-1}$. We show in Appendix D that the RB decays to $\frac{1}{d}$.

V. SIGNATURES OF NON-MARKOVIANITY

Several methods have been introduced to reliably identify and quantify non-Markovianity in quantum systems [40,42–44], information backflow from environment to system [45], divisibility of the evolution map [46], etc. However, these methods are considered independently from RB experiments. Here, we show that RB experiments readily provide distinguishability measures such as the fidelity and trace distance (BLP measure [43]) to determine the presence of non-Markovianity in the system.

In particular, we propose to measure the trace distance between the evolution of orthogonal states ($|0\rangle$ and $|1\rangle$) at varying sequence lengths, a measure that must be contractive, or decrease monotonically, for Markovian systems as both states depolarize to the same maximally mixed state. The evolution map here is one instance of the non-Markovian model in Fig. 1, with random unitary gates.

$$D\big(\rho_{{\rm sys},k}^{|0\rangle}, \rho_{{\rm sys},k}^{|1\rangle}\big) = \tfrac{1}{2}\,\mathrm{tr}\,\big|\rho_{{\rm sys},k}^{|0\rangle} - \rho_{{\rm sys},k}^{|1\rangle}\big|. \tag{20}$$

For each random circuit instance, we observed distinct time steps displaying an increase in trace distance (see Fig. 4), a clear indication of the presence of non-Markovianity. In contrast, the trace distance is monotonically decreasing for a Markovian circuit. The inset in Fig. 4 shows the distribution of the change in trace distance over many circuit realizations.

VI. CONCLUSIONS AND OUTLOOK

We studied a system interacting with an environment with a long quantum memory, resulting in a non-Markovian dynamics of the system. We found a drastically different RB decay with non-Markovian noise compared to the Markovian case, which also differs qualitatively at early depths. Although they both tail off exponentially, non-Markovian decays in our model are much slower than ones for Markovian systems, under the same parameters. We showed this by considering a simplified, exactly solvable model of qudits interacting with a bosonic bath. By determining the signatures of a non-Markovian decay, we provide guidance to identify these effects in common characterization experiments. The computation in this work was possible because the eigenvectors of the Hamiltonian could be solved analytically. In general, this simplification is not possible, making it important to determine the universality of these results to other models of non-Markovian quantum systems. This work opens interesting avenues for research to theoretically relate the source of the nonexponential behavior to the details of the system-bath interaction, paving the way for more precise noise characterization.

ACKNOWLEDGMENTS

We thank Xiao Xiao and Anantha Rao for useful discussions. This work was supported in part by ARO Grant No. W911NF-23-1-0258.

DATA AVAILABILITY

No data were created or analyzed in this study.

APPENDIX A: NON-MARKOVIAN EVOLUTION

Our objective is to find the average final state of the system, after k layers, averaged over the unitary group $\mathcal{U}(d)$. Each Hamiltonian interaction has a duration t (see Fig. 1).

$$\mathbb{E}_U[\rho_{s,k}] = \mathrm{tr}_E(\mathbb{E}_U[\mathcal{U}^{-1} \circ \mathcal{E}_H \circ \mathcal{U}_k \cdots \circ \mathcal{E}_H \circ \mathcal{U}_1 (\rho_s \otimes \rho_{\mathrm{env}})]). \tag{A1}$$

Since only linear operations are involved without loss of generality, we can assume that the initial state is a product state. The results also hold for mixed states. We compute the average over unitaries using the expression for Haar average shown below. By definition, this is also valid for any 2-design, and therefore the Clifford group, which is of interest in RB. Using

$$\int_{\mathcal{U}(d)} d\eta(U) U^\dagger A U \rho U^\dagger B U = \frac{\mathrm{tr}\,(AB)\,\mathrm{tr}\,(\rho)}{d}\frac{\mathbb{I}}{d} + \left(\frac{d\,\mathrm{tr}\,(A)\,\mathrm{tr}\,(B) - \mathrm{tr}\,(AB)}{d(d^2-1)}\right)\left(\rho - \mathrm{tr}\,(\rho)\frac{\mathbb{I}}{d}\right), \tag{A2}$$

and the projectors $P_0 = |0\rangle\langle 0|$ and $P_1 = |1\rangle\langle 1|$, a single layer of twirling gives us a depolarizing channel

$$\mathbb{E}_U[U^{-1} P_p U \rho_s U^\dagger P_q U^{-1\dagger}] = \left(\frac{2}{3}\delta_{pq} - \frac{1}{3}\right)\mathrm{tr}\,(\rho_s)\frac{\mathbb{I}}{2} + \left(\frac{2-\delta_{pq}}{6}\right)\rho_s. \tag{A3}$$

For k layers, let us define $\mathcal{M}_k(\mathbf{p},\mathbf{q})$ as the state of system determined by projector sequences $\mathbf{p} = (p_1,\ldots,p_k)$ and $\mathbf{q} = (q_1,\ldots,q_k)$. Then, the expectation value is

$$\begin{aligned}
\mathbb{E}_U\big[\mathcal{M}_k(\mathbf{p},\mathbf{q})\big] &\equiv \mathbb{E}_U[U^{-1} P_{p_k} U_k \cdots P_{p_1} U_1 \rho_s U_1^\dagger P_{q_1} \cdots U_k^\dagger P_{q_k} U^{-1\dagger}] \\
&= \mathbb{E}_{[k-1]}\big[\mathbb{E}_k\big[\tilde{U}_k^\dagger P_{p_k} \tilde{U}_k \mathcal{M}_{k-1}\, \tilde{U}_k^\dagger P_{q_k} \tilde{U}_k\big]\big] \\
&= \mathbb{E}_{[k-1]}\left[\left(\frac{2}{3}\delta_{p_k q_k} - \frac{1}{3}\right)\mathrm{tr}\,(\mathcal{M}_{k-1})\frac{\mathbb{I}}{2} + \left(\frac{2-\delta_{p_k q_k}}{6}\right)\mathcal{M}_{k-1}\right],
\end{aligned} \tag{A4}$$

where $\mathcal{M}_i = \tilde{U}_i^\dagger P_{p_i} \tilde{U}_i \mathcal{M}_{i-1} \tilde{U}_i^\dagger P_{q_i} \tilde{U}_i$ is recursively defined and $\mathcal{M}_0 = \rho_s$. We used $U^{-1} = U^\dagger$, and inserted unitaries and their inverses in the first step to separate and cast the twirling of different unitaries into the form given by Eq. (A2). We denote $\prod_{i=0}^{m-1} U_{m-i} \equiv \tilde{U}_m$ and the expectation $\mathbb{E}_{U_1,\ldots,U_i} \equiv \mathbb{E}_{[i]}$, making $\mathbb{E}_{[k]} = \mathbb{E}_U$.

Taking trace on both sides and denoting δ_{p_i,q_i} as δ_i,

$$\mathbb{E}_{[k]}[\mathrm{tr}\,(\mathcal{M}_k)] = \frac{\delta_k}{2}\,\mathbb{E}_{[k-1]}[\mathrm{tr}\,(\mathcal{M}_{k-1})] = \prod_{j=1}^{k}\frac{\delta_j}{2}\;\mathrm{tr}\,(\mathcal{M}_0) = \frac{1}{2^k}\left(\prod_{j=1}^{k}\delta_j\right)\;\mathrm{tr}\,(\rho_s). \tag{A5}$$

Substituting this as the first term of Eq. (A4),

$$\begin{aligned}
\mathbb{E}_{[k]}[\mathcal{M}_k] &= \left(\frac{2}{3}\delta_k - \frac{1}{3}\right)\mathbb{E}_{[k-1]}[\mathrm{tr}\,(\mathcal{M}_{k-1})]\;\mathrm{tr}\,(\rho_s)\frac{\mathbb{I}}{2} + \left(\frac{2-\delta_{p_k q_k}}{6}\right)\mathbb{E}_{[k-1]}[\mathcal{M}_{k-1}] \\
&= \frac{1}{3}(2\delta_k - 1)\left(\prod_{j=1}^{k-1}\frac{\delta_j}{2}\right)\mathrm{tr}\,(\rho_s)\frac{\mathbb{I}}{2} + \frac{1}{3}\left(1 - \frac{\delta_k}{2}\right)\mathbb{E}_{[k-1]}[\mathcal{M}_{k-1}].
\end{aligned} \tag{A6}$$

Solving the recursive relation, we would have the depolarizing channel whose coefficients need to be determined. Defining $\gamma\,(\mathbf{p},\mathbf{q}) \equiv \prod_{i=1}^{k}(1 - \frac{\delta_i}{2})$,

$$\mathbb{E}_{[k]}[\mathcal{M}_k] = \left(\Delta(\mathbf{p},\mathbf{q})\;\mathrm{tr}\,(\rho_s)\frac{\mathbb{I}}{2} + \frac{1}{3^k}\gamma\,(\mathbf{p},\mathbf{q})\,\rho_s\right), \tag{A7}$$

where the unknown $\Delta(\mathbf{p},\mathbf{q})$ can be determined by taking trace on both sides and using Eq. (A5),

$$\frac{1}{2^k}\left(\prod_{j=1}^{k}\delta_j\right)\;\mathrm{tr}\,(\rho_s) = \;\Delta(\mathbf{p},\mathbf{q})\;\mathrm{tr}\,(\rho_s) + \frac{1}{3^k}\gamma\,(\mathbf{p},\mathbf{q})\;\mathrm{tr}\,(\rho_s), \tag{A8}$$

which gives us

$$\Delta(\mathbf{p},\mathbf{q}) = \frac{1}{2^k}\prod_{j=1}^{k}\delta_j - \frac{1}{3^k}\gamma\,(\mathbf{p},\mathbf{q}). \tag{A9}$$

Writing $\prod_{j=1}^{k}\delta_j$ as $\delta_{\mathbf{p},\mathbf{q}}$, we have

$$\mathbb{E}_U[\mathcal{M}_k(\mathbf{p},\mathbf{q})] = \frac{1}{3^k}\gamma\,(\mathbf{p},\mathbf{q})\left(\rho_s - \mathrm{tr}\,(\rho_s)\frac{\mathbb{I}}{2}\right) + \frac{1}{2^k}\,\delta_{\mathbf{p},\mathbf{q}}\;\mathrm{tr}\,(\rho_s)\frac{\mathbb{I}}{2}. \tag{A10}$$

Plugging that into Eq. (14) and expressing $\gamma\,(\mathbf{p},\mathbf{q}) = (\frac{1}{2})^{k-d(\mathbf{p},\mathbf{q})}$ in terms of the Hamming distance $d(\mathbf{p},\mathbf{q})$ between the strings $\mathbf{p}$ and $\mathbf{q}$, we find that the average final state is

$$\mathbb{E}_U[\rho_{s,k}] = \frac{\mathbb{I}}{2} + \frac{1}{6^k}\sum_{\mathbf{p},\mathbf{q}} 2^{d(\mathbf{p},\mathbf{q})}\,\mathrm{tr}\,(\mathcal{H}(\mathbf{p})\,\rho_{\mathrm{env}}\,\mathcal{H}^{\dagger}(\mathbf{q}))\left(\rho_s - \frac{\mathbb{I}}{2}\right). \tag{A11}$$

APPENDIX B: MARKOVIAN EVOLUTION

When the state of the environment is refreshed before every interaction with the system, the averaged state of the system after k layers, similar to the previous calculation, is

$$\begin{aligned}
\mathbb{E}_U\left[\rho_{s,k}^{(M)}\right] &= \sum_{\mathbf{p},\mathbf{q}\in\{0,1\}^{\otimes k}} \mathbb{E}_U[\mathcal{M}_k(\mathbf{p},\mathbf{q})]\prod_{j=1}^{k}\mathrm{tr}\,(e^{-iH_{p_j}t}\rho_{\mathrm{env}}e^{iH_{q_j}t}) \\
&= \sum_{\mathbf{p},\mathbf{q}}\frac{1}{3^k}\gamma(\mathbf{p},\mathbf{q})\left(\rho_s - \mathrm{tr}\,(\rho_s)\frac{\mathbb{I}}{2}\right)\prod_{j=1}^{k}\mathrm{tr}\,(e^{-iH_{p_j}t}\rho_{\mathrm{env}}e^{iH_{q_j}t}) + \sum_{\mathbf{p}}\frac{1}{2^k}\;\mathrm{tr}\,(\rho_s)\;\mathrm{tr}\,(\rho_{\mathrm{env}})^k\frac{\mathbb{I}}{2} \\
&= \frac{1}{3^k}(\mathrm{tr}\,(\rho_{\mathrm{env}}) + 2\;\mathrm{tr}\,(\cos((H_0-H_1)\Delta t)\,\rho_{\mathrm{env}}))^k\left(\rho_s - \mathrm{tr}\,(\rho_s)\frac{\mathbb{I}}{2}\right) + \mathrm{tr}\,(\rho_s)\;\mathrm{tr}\,(\rho_{\mathrm{env}})^k\frac{\mathbb{I}}{2}.
\end{aligned} \tag{B1}$$

When $\mathrm{tr}\,(\rho_{\mathrm{env}}) = 1$, the prefactor $\frac{1}{3^k}\,(1 + 2\;\mathrm{tr}\,(\cos((H_0 - H_1)t)\rho_{\mathrm{env}}))^k$ exponentially decays with depth and therefore the system approaches the maximally mixed state $\frac{\mathbb{I}}{2}$.

Using $\mathrm{tr}\,(\rho_{\mathrm{env}}) = 1$, $\mathrm{tr}\,(\rho_s) = 1$, and $H_0 - H_1 = 2gx$, RB output is

$$f_k^M(\rho_s,\rho_{\mathrm{env}}) = \mathrm{tr}\left(\mathbb{E}_U\left[\rho_{s,k}^{(M)}\right]\rho_s\right) = \frac{1}{2} + \frac{1}{2}\left(\frac{1 + 2\;\mathrm{tr}\,(\cos(2gx\Delta t)\rho_{\mathrm{env}})}{3}\right)^k. \tag{B2}$$

APPENDIX C: XI MODEL

Consider a binary sequence $(u_1,\ldots,u_k)$ with u_i representing the gate at the ith position: 0 for gate $\mathbb{I}$ and 1 for gate X. Then, if the number of X gates, i.e., $\sum_i u_i$, is equal to N_X, the final state can be written as

$$U_k e^{-iHt}\cdots U_1 e^{-iHt}\,\rho_{\mathrm{in}}\,U_1^{\dagger}e^{iHt}\cdots U_k^{\dagger}e^{iHt}. \tag{C1}$$

Let us define

$$H_s = (-1)^s\,g\,(a + a^{\dagger})\,Z + \omega a^{\dagger}a\,\mathbb{I}, \tag{C2}$$

$\mathcal{H}_s = \exp\,(-iH_s\Delta t)$, and $r_j = \sum_{i=j}^{k} u_i$. Moving all the X operators toward the initial state,

$$\mathcal{H}_0\mathcal{H}_{r_k}\mathcal{H}_{r_{k-1}}\cdots\mathcal{H}_{r_2}X^{N_X}\,\rho_{\mathrm{in}}\,X^{N_X}\mathcal{H}_{r_2}^{\dagger}\cdots\mathcal{H}_{r_k}^{\dagger}\mathcal{H}_0^{\dagger}. \tag{C3}$$

Because Z acts only on the system, we can expand $\mathcal{H}_s$ using the projectors on the system space as

$$\begin{aligned}
\mathcal{H}_s &= P_0\otimes e^{-i\,((-1)^s\,g\,(a+a^{\dagger})+\omega a^{\dagger}a)\Delta t} + P_1\otimes e^{-i\,(-(-1)^s\,g\,(a+a^{\dagger})+\omega a^{\dagger}a)\Delta t} \\
&= \sum_{p\in\{0,1\}} P_p\otimes e^{-i\,((-1)^{s+p}\,g\,(a+a^{\dagger})+\omega a^{\dagger}a)\Delta t} \\
&\equiv \sum_{p\in\{0,1\}} P_p\otimes\tilde{\mathcal{H}}_{s+p},
\end{aligned} \tag{C4}$$

defining $\tilde{\mathcal{H}}$ that acts only on the environment Hilbert space. To determine the average output, we can sequentially average from u_1 through u_k, each drawn from the set $\{0, 1\}$ uniformly randomly. One instance of averaging over the gate set $\{X, \mathbb{I}\}$ gives us

$$S_1 = \mathcal{H}_0\,\rho_{\text{in}}\,\mathcal{H}_0^\dagger + \mathcal{H}_1\,\rho_{\text{in}}\,\mathcal{H}_1^\dagger = \sum_{s\in\{0,1\}} \mathcal{H}_s\,\rho_{\text{in}}\,\mathcal{H}_s^\dagger; \tag{C5}$$

using Eq. (C4),

$$S_1 = \sum_{s,p,q\in\{0,1\}} (P_p \otimes \mathcal{H}_{s+p})\,\rho_{\text{in}}\,(P_q \otimes \mathcal{H}_{s+q}^\dagger), \tag{C6}$$

leading to four branches after one layer similar to the Clifford non-Markovian case in Appendix A. After k layers, we have 4^k trajectories labeled here using three k-length bit strings $\mathbf{s}$, $\mathbf{p}$, $\mathbf{q}$ that can be similarly numerically summed as in the Clifford case. The averaged final state is

$$S_k = \sum_{\mathbf{s},\mathbf{p},\mathbf{q}} \left(P_{p_k} \otimes \mathcal{H}_{s_k+p_k}\right)\cdots\left(P_{p_1} \otimes \mathcal{H}_{s_1+p_1}\right)\rho_{\text{in}}\left(P_{q_1} \otimes \mathcal{H}_{s_1+q_1}\right)\cdots\left(P_{q_k} \otimes \mathcal{H}_{s_k+q_k}\right). \tag{C7}$$

APPENDIX D: MULTIQUBIT SYSTEMS AND MULTIMODE BATHS

Consider an n-qubit system interacting with a multimode bosonic environment. Let us start with a product state $\rho_{\text{SE}} = \rho_s \otimes \rho_{\text{env}}$ and apply a sequence of n-qubit unitary operations $U_1, \ldots, U_k, U_{\text{inv}}$, where the dimension of the system $d = 2^n$, $U_i \in \mathbb{U}_d$, and $U_{\text{inv}} = (U_1 \cdots U_k)^{-1}$. We want to compute the average final state

$$\mathbb{E}_U[\rho_{s,k}] = \sum_{\substack{p_i,q_i\in\{0,1\}^{\otimes n}\\ 1\leqslant i\leqslant k}} \mathbb{E}_U\left[\tilde{U}_k^\dagger P_{p_k}\tilde{U}_k\cdots\tilde{U}_1^\dagger P_{p_1}\tilde{U}_1\rho_s\tilde{U}_1^\dagger P_{q_1}\tilde{U}_1\cdots\tilde{U}_k^\dagger P_{q_k}\tilde{U}_k\right] \otimes \mathcal{H}(\mathbf{p})\rho_{\text{env}}\mathcal{H}^\dagger(\mathbf{q}), \tag{D1}$$

where $\mathcal{H}(\mathbf{p}) = e^{-iH_{\mathbf{p}}t}$, and as defined in the main text $H_p = \sum_{i=1}^m \omega_i a_i^\dagger a_i + w(p)\,g_{ij}(a_i + a_i^\dagger)$, using the weighted sum of a bit string $w(q) \equiv \sum_{j=1}^n (-1)^{q_j}$.

Similar to the single-qubit analysis, Haar average at $d = 2^n$ is

$$\begin{aligned}\mathbb{E}_U[U^\dagger P_p U\,\mathcal{M}\,U^\dagger P_q U] &= \frac{\delta_{pq}}{d}\,\text{tr}\,(\mathcal{M})\frac{\mathbb{I}}{d} + \frac{1}{d^2-1}\left(1-\frac{\delta_{pq}}{d}\right)\left(\mathcal{M} - \text{tr}\,(\mathcal{M})\frac{\mathbb{I}}{d}\right)\\ &= \frac{d\delta_{pq}-1}{d^2-1}\,\text{tr}\,(\mathcal{M})\frac{\mathbb{I}}{d} + \frac{1}{d^2-1}\left(1-\frac{\delta_{pq}}{d}\right)\mathcal{M}.\end{aligned} \tag{D2}$$

Defining $\mathcal{M}_k(\mathbf{p}, \mathbf{q})$ as before,

$$\mathbb{E}_U[\text{tr}\,(\mathcal{M}_k(\mathbf{p},\mathbf{q}))] = \prod_{j=1}^k \frac{\delta_j}{d}\;\text{tr}\,(\rho_s), \tag{D3}$$

we have

$$\mathbb{E}_U[\mathcal{M}_k(\mathbf{p},\mathbf{q})] = \Delta(\mathbf{p},\mathbf{q})\;\text{tr}\,(\rho_s)\frac{\mathbb{I}}{d} + \frac{1}{(d^2-1)^k}\prod_{j=1}^k\left(1-\frac{\delta_j}{d}\right)\rho_s, \tag{D4}$$

$$\Delta(\mathbf{p},\mathbf{q}) = \frac{1}{d^k}\prod_{j=1}^k\delta_j - \frac{1}{(d^2-1)^k}\prod_{j=1}^k\left(1-\frac{\delta_j}{d}\right). \tag{D5}$$

If $\text{tr}\,(\rho_s) = \text{tr}\,(\rho_{\text{env}}) = 1$, and if the system begins in the ground state, RB output is

$$\frac{1}{d} + \frac{1}{(d^2-1)^k}\sum_{\mathbf{p},\mathbf{q}}\left(1-\frac{1}{d}\right)^{1+k-d(\mathbf{p},\mathbf{q})}\text{tr}\,(\mathcal{H}(\mathbf{p})\rho_{\text{env}}\mathcal{H}^\dagger(\mathbf{q})). \tag{D6}$$

[1] J. Helsen, J. J. Wallman, S. T. Flammia, and S. Wehner, Multiqubit randomized benchmarking using few samples, Phys. Rev. A **100**, 032304 (2019).

[2] J. Helsen, X. Xue, L. M. K. Vandersypen, and S. Wehner, A new class of efficient randomized benchmarking protocols, npj Quantum Inf. **5**, 71 (2019).

[3] A. Carignan-Dugas, J. J. Wallman, and J. Emerson, Characterizing universal gate sets via dihedral benchmarking, Phys. Rev. A **92**, 060302(R) (2015).

[4] W. G. Brown and B. Eastin, Randomized benchmarking with restricted gate sets, Phys. Rev. A **97**, 062323 (2018).

[5] A. K. Hashagen, S. T. Flammia, D. Gross, and J. J. Wallman, Real randomized benchmarking, Quantum **2**, 85 (2018).

[6] J. Helsen, S. Nezami, M. Reagor, and M. Walter, Matchgate benchmarking: Scalable benchmarking of a continuous family of many-qubit gates, Quantum **6**, 657 (2022).

[7] J. Claes, E. Rieffel, and Z. Wang, Character randomized benchmarking for non-multiplicity-free groups with applications to subspace, leakage, and matchgate randomized benchmarking, PRX Quantum **2**, 010351 (2021).

[8] K. Young, S. Bartlett, R. Blume-Kohout, J. Gamble, D. Lobser, P. Maunz, E. Nielsen, T. Proctor, M. Revelle, and K. Rudinger, *Diagnosing and Destroying Non-Markovian Noise*, Report No. SAND2020-10118R (Sandia National Laboratories, Albuquerque, NM, 2020).

[9] K. X. Wei, E. Pritchett, D. M. Zajac, D. C. McKay, and S. Merkel, Characterizing non-Markovian off-resonant errors in quantum gates, Phys. Rev. Appl. **21**, 024018 (2024).

[10] D. Aharonov, A. Kitaev, and J. Preskill, Fault-tolerant quantum computation with long-range correlated noise, Phys. Rev. Lett. **96**, 050504 (2006).

[11] G. A. L. White, C. D. Hill, F. A. Pollock, L. C. L. Hollenberg, and K. Modi, Demonstration of non-Markovian process characterisation and control on a quantum processor, Nat. Commun. **11**, 6301 (2020).

[12] M. J. Gullans, M. Caranti, A. R. Mills, and J. R. Petta, Compressed gate characterization for quantum devices with time-correlated noise, PRX Quantum **5**, 010306 (2024).

[13] B. Gulácsi and G. Burkard, Signatures of non-Markovianity of a superconducting qubit, Phys. Rev. B **107**, 174511 (2023).

[14] J. F Kam, S. Gicev, K. Modi, A. Southwell, and M. Usman, Detrimental non-Markovian errors for surface code memory, Quantum Sci. Technol. **10**, 035060 (2025).

[15] P. Groszkowski, A. Seif, J. Koch, and A. A. Clerk, Simple master equations for describing driven systems subject to classical non-Markovian noise, Quantum **7**, 972 (2023).

[16] A. Seif, Y.-X. Wang, and A. A. Clerk, Distinguishing between quantum and classical markovian dephasing dissipation, Phys. Rev. Lett. **128**, 070402 (2022).

[17] K. Huang, D. Farfurnik, A. Seif, M. Hafezi, and Y.-K. Liu, Random pulse sequences for qubit noise spectroscopy, Phys. Rev. Appl. **23**, 054090 (2025).

[18] G. D. Berk, A. J. P. Garner, B. Yadin, K. Modi, and F. A. Pollock, Resource theories of multi-time processes: A window into quantum non-Markovianity, Quantum **5**, 435 (2021).

[19] G. D. Berk, S. Milz, F. A. Pollock, and K. Modi, Extracting quantum dynamical resources: Consumption of non-Markovianity for noise reduction, npj Quantum Inf. **9**, 104 (2023).

[20] V. B. Sabale, N. R. Dash, A. Kumar, and S. Banerjee, Facets of correlated non-Markovian channels, Ann. Phys. **536**, 2400151 (2024).

[21] I. de Vega and D. Alonso, Dynamics of non-Markovian open quantum systems, Rev. Mod. Phys. **89**, 015001 (2017).

[22] P. Figueroa-Romero, K. Modi, R. J. Harris, T. M. Stace, and M.-H. Hsieh, Randomized benchmarking for non-Markovian noise, PRX Quantum **2**, 040351 (2021).

[23] L. Viola and S. Lloyd, Dynamical suppression of decoherence in two-state quantum systems, Phys. Rev. A **58**, 2733 (1998).

[24] L. Viola, E. Knill, and S. Lloyd, Dynamical decoupling of open quantum systems, Phys. Rev. Lett. **82**, 2417 (1999).

[25] L. Viola and E. Knill, Robust dynamical decoupling of quantum systems with bounded controls, Phys. Rev. Lett. **90**, 037901 (2003).

[26] M. Burgelman, N. Wonglakhon, D. N. Bernal-García, G. A. Paz-Silva, and L. Viola, Limitations to dynamical error suppression and gate-error virtualization from temporally correlated nonclassical noise, PRX Quantum **6**, 010323 (2025).

[27] G. A. L. White, F. A. Pollock, L. C. L. Hollenberg, K. Modi, and C. D. Hill, Non-markovian quantum process tomography, PRX Quantum **3**, 020344 (2022).

[28] D. Loss and D. P. DiVincenzo, Quantum computation with quantum dots, Phys. Rev. A **57**, 120 (1998).

[29] H. Bluhm, S. Foletti, I. Neder, M. Rudner, D. Mahalu, V. Umansky, and A. Yacoby, Dephasing time of GaAs electron-spin qubits coupled to a nuclear bath exceeding 200 μs, Nat. Phys. **7**, 109 (2010).

[30] N. A. Kamar, D. A. Paz, and M. F. Maghrebi, Spin-boson model under dephasing: Markovian versus non-Markovian dynamics, Phys. Rev. B **110**, 075126 (2024).

[31] More generally, the gate set may be the Clifford group or any unitary 2-design approximating the Haar distribution. If the twirling group has multiple irreducible representations on the traceless operator subspace, the resulting average sequence fidelity will in general exhibit a sum of exponentials rather than a single-exponential decay.

[32] J. Emerson, R. Alicki, and K. Życzkowski, Scalable noise estimation with random unitary operators, J. Opt. B: Quantum Semiclassical Opt. **7**, S347 (2005).

[33] E. Knill, D. Leibfried, R. Reichle, J. Britton, R. B. Blakestad, J. D. Jost, C. Langer, R. Ozeri, S. Seidelin, and D. J. Wineland, Randomized benchmarking of quantum gates, Phys. Rev. A **77**, 012307 (2008).

[34] G. H. Low and N. Wiebe, Hamiltonian simulation in the interaction picture, arXiv:1805.00675.

[35] K. Sharma and M. C. Tran, Hamiltonian simulation in the interaction picture using the magnus expansion, arXiv:2404.02966.

[36] If $U' \equiv e^{-iH_{\rm sys}\Delta t}\,U$ or $U' \equiv U\,e^{-iH_{\rm sys}\Delta t}$, where U is sampled from the Haar measure and $e^{-iH_{\rm sys}\Delta t}$ is the system evolution, then U' is statistically indistinguishable from U due to the left and right invariance of the Haar measure. That is, $\int dU U^\dagger \Lambda U = \int dU\, U^\dagger V^\dagger \Lambda V U = \int dU\, V^\dagger U^\dagger \Lambda U V$.

[37] G. Cenedese, G. Benenti, and M. Bondani, Correcting coherent errors by random operation on actual quantum hardware, Entropy **25**, 324 (2023).

[38] G. Feng, J. J. Wallman, B. Buonacorsi, F. H. Cho, D. K. Park, T. Xin, D. Lu, J. Baugh, and R. Laflamme, Estimating the coherence of noise in quantum control of a solid-state qubit, Phys. Rev. Lett. **117**, 260501 (2016).

[39] A. Hashim, R. K. Naik, A. Morvan, J.-L. Ville, B. Mitchell, J. M. Kreikebaum, M. Davis, E. Smith, C. Iancu, K. P. O'Brien, I. Hincks, J. J. Wallman, J. Emerson, and I. Siddiqi, Randomized compiling for scalable quantum computing on a noisy superconducting quantum processor, Phys. Rev. X **11**, 041039 (2021).

[40] A. Rivas, S. F. Huelga, and M. B. Plenio, Entanglement and non-markovianity of quantum evolutions, Phys. Rev. Lett. **105**, 050403 (2010).

[41] There are other reasons why the average sequence fidelity may fail to exhibit single-exponential decay even when the gate set would permit it, such as time-dependent or drifting noise

channels. In our setting, however, the interaction unitary is fixed and the Clifford gate set is used, so any deviation from single-exponential decay can be attributed to non-Markovian effects in the dynamics.

[42] A. Rivas, S. F. Huelga, and M. B. Plenio, Quantum non-Markovianity: Characterization, quantification and detection, Rep. Prog. Phys. **77**, 094001 (2014).

[43] H.-P. Breuer, E.-M. Laine, and J. Piilo, Measure for the degree of non-Markovian behavior of quantum processes in open systems, Phys. Rev. Lett. **103**, 210401 (2009).

[44] S. M. Hosseiny, J. Seyed-Yazdi, and M. Norouzi, Witness of non-Markovian dynamics based on Bhattacharyya quantum distance, Sci. Rep. **14**, 18261 (2024).

[45] E.-M. Laine, J. Piilo, and H.-P. Breuer, Measure for the non-Markovianity of quantum processes, Phys. Rev. A **81**, 062115 (2010).

[46] D. Chruściński, A. Kossakowski, and A. Rivas, Measures of non-Markovianity: Divisibility versus backflow of information, Phys. Rev. A **83**, 052128 (2011).